On the Universality of Inversion Layer Mobility in Si MOSFET's: Part II—Effects of Surface Orientation

Shin-ichi Takagi, *Member, IEEE,* Akira Toriumi, Masao Iwase, and Hiroyuki Tango

***Abstract*—This paper reports the studies of the inversion layer mobilities in n-channel MOSFET's fabricated on Si wafers with three surface orientations ((100), (110), and (111)) from the viewpoint of the universal relationship against the effective field, $E_{\rm eff}(= q(N_{\rm dpl} + \eta \cdot N_s)/\varepsilon Si)$. It is found that the universality does hold for the electron mobilities on (110) and (111), when the value of η is taken to be 1/3, different from the electron mobility on (100), where η is 1/2. Also, the $E_{\rm eff}$ dependence of the electron mobility is found to differ among (100), (110), and (111) surfaces. This is attributed to the differences in the $E_{\rm eff}$ dependence of the mobility limited by surface roughness scattering among the orientations.**

The origins of $E_{\rm eff}$ and η are discussed on the basis of the relaxation time approximation for a 2DEG (2-dimensional electron gas). While the surface orientation dependence of η in phonon scattering can be understood in terms of the subband occupation, it is found that the theoretical formulation of surface roughness scattering, used currently, needs to be refined in order to explain the differences in $E_{\rm eff}$ dependence and the value of η among the three orientations.

I. Introduction

The universal relationship for the effective field, $E_{\rm eff}$ is quite useful for characterizing the inversion layer mobility in Si MOSFET's with various device parameters [1]–[8]. In fact, we have confirmed in the companion paper [8] that the universal relationship does hold for both the electron and hole mobilities on (100) surface up to the substrate impurity concentration of 10^{18} cm^{-3}, except for at low surface carrier concentrations, where Coulomb scattering becomes dominant. However, there remain some unclear points regarding the universality, such as the origin of the universality, the physical meanings of $E_{\rm eff}(= q \cdot (N_{\rm dpl} + \eta \cdot N_s)/\varepsilon_{\rm Si})$, the parameter η and the $E_{\rm eff}$ dependences of the universal curve.

In this paper the effect of the surface orientation on the universality is studied from the view point of changing the subband structure, in order to shed light on these problems. It has already been reported [4], [5] that the value of η is different between electrons and holes on (100) surface. Also, the companion paper [8] demonstrated in case of (100) surface that the $E_{\rm eff}$ dependence of the electron mobility is different from that of the hole mobility. These facts suggest that electronic properties of a 2DEG such as subband structure can play an important role in the universality. While the surface orientation is known to change the subband structure [9]–[11], the universal relationship of the inversion layer mobility on surface orientation different from (100) has not been so far studied at all. In this paper the universality of the electron mobility on (110) and (111) surfaces are investigated. Based on these experimental results, the physical origins of $E_{\rm eff}$, η, and $E_{\rm eff}$ dependence of the universal curve the discussed in terms of scattering mechanism in the inversion layer.

Manuscript received June 3, 1994. The review of this paper was arranged by Associate Editor K. Tada.

S. Takagi is with the Solid State Electronics Laboratory, Stanford University, Stanford, CA 94305 USA.

A. Toriumi, M. Iwase, and H. Tango are with the ULSI Research Laboratories, Research & Development Center, Toshiba Corporation, 1 Kamukai Toshiba-cho, Saiwai-Ku, Kawasaki 210, Japan.

IEEE Log Number 9405894.

II. Experimental Results

A. Universal Relationship

N-channel MOSFET's used in this study were fabricated on (100), (110) and (111) Si wafers. The fabrication process of the MOSFET's, the device dimension and the measurement method were the same as those in the companion paper [8]. The current flow direction in the channel was parallel to $\langle 011 \rangle$ axis on the three surface orientations. In order to examine the universal relationship, it is necessary to find an appropriate value of η. As shown in the companion paper [8], the universal relationship for the electron and hole mobilities on (100) surface is obtained by taking the value of η to be 1/2 and 1/3, respectively. It is, however, still nuclear whether the universal relationship can hold or not for the electron mobilities on (110) and (111). Thus, the existence of the universal relationship is examined by regarding the value of η as a parameter and comparing the mobilities with the different substrate impurity concentration.

Figs. 1 and 2 show the relationship between $E_{\rm eff}$ and the electron mobilities at 300 K on (110) and (111), respectively, as a parameter of substrate impurity concentration. Here, the value of η is taken to be 1/2 in Fig. 1(a) and Fig. 2(a) and 1/3 in Fig. 1(b) and Fig. 2(b). It is clearly observed that the universality on the (110) and (111) surfaces can be well maintained when $\eta = 1/3$ instead of 1/2 for the electron mobility on (100). Figs. 3 and 4 show the $E_{\rm eff}$ dependences of the electron mobility at 77 K on (110) and (111) when $\eta = 1/3$. It is found that η should be also 1/3 at 77 K to obtain the universality.

The value of η, which provides the universal relationship of the mobility, have been summarized in Table I. It should be noted that η for the electron mobility is not necessarily 1/2 and is dependent on the surface orientation. The fact that η is dependent on the surface orientation suggests that the subband structure can significantly affect η. The relationship between η and the subband structure will be discussed in Section III.

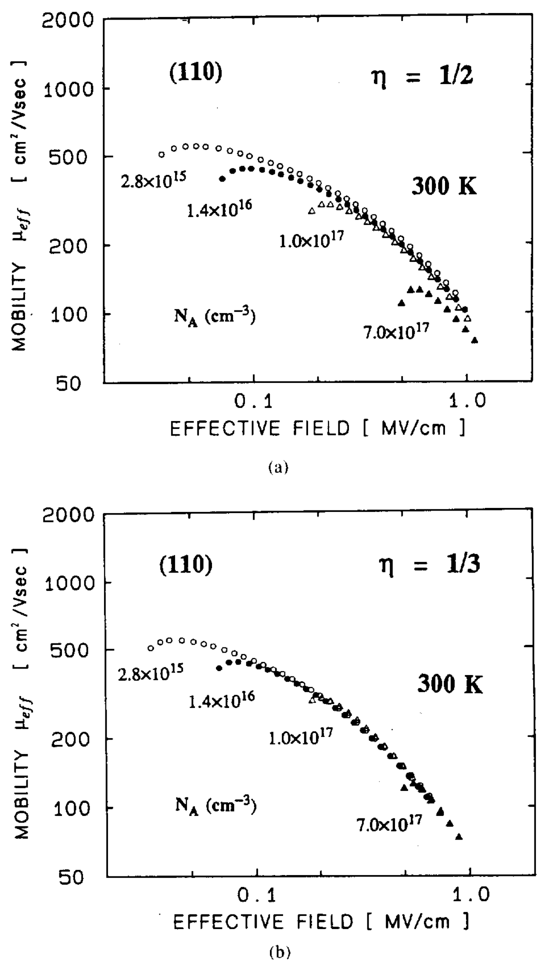

Fig. 1. Electron mobility in inversion layer on (110) at 300 K versus effective field, $E_{\rm eff}$, as a parameter of substrate acceptor concentration, N_A. Here, $E_{\rm eff}$ is defined by $E_{\rm eff} = q \cdot (N_{\rm dpl} + \eta N_s)/\varepsilon_{\rm Si}$ with η of (a) 1/2 and (b) 1/3.

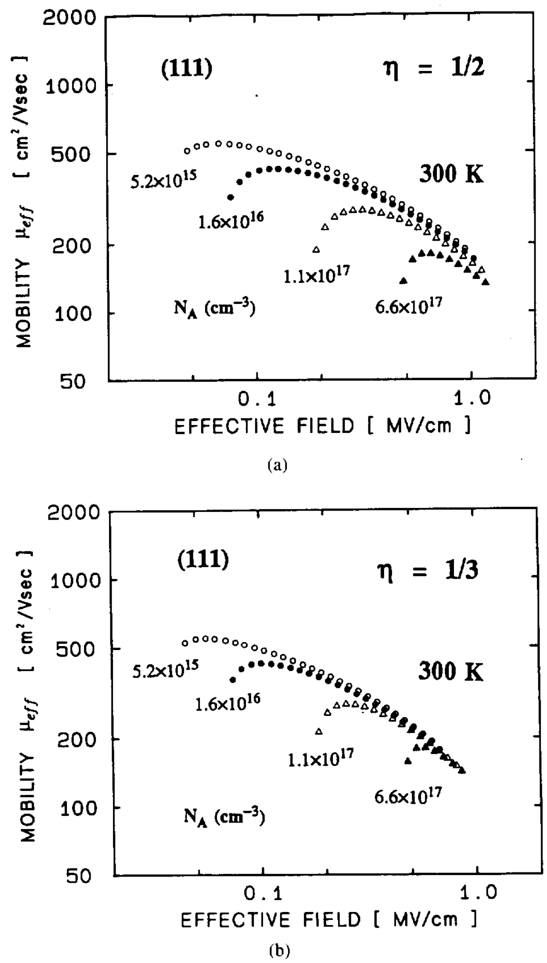

Fig. 2. Electron mobility in inversion layer on (111) at 300 K versus effective field, $E_{\rm eff}$ as a parameter of substrate acceptor concentration, N_A. Here, $E_{\rm eff}$ is defined by $E_{\rm eff} = q \cdot (N_{\rm dpl} + \eta N_s)/\varepsilon_{\rm Si}$ with η of (a) 1/2 and (b) 1/3.

B. Effective Field Dependence of Universal Curves on (100), (110), and (111)

The surface orientation dependence of the mobility has been mainly attributed to the difference in the effective mass to far [11]. However, the fact that the $E_{\rm eff}$ dependence is different among the three surface orientations (see Figs. 1, 2 and Fig. 1 in [8]) cannot be explained only by the different effective mass. In particular, the $E_{\rm eff}$ dependences on (110) and (111) in high $E_{\rm eff}$ region at 77 K are observed to be rather weaker than that on (100), as shown in Figs. 3 and 4, indicating that the mobility limited by surface roughness scattering, $\mu_{\rm sr}$, differs considerably among the three surface orientations.

Figs. 5 and 6 show the temperature dependences of the electron mobility on (110) and (111) surfaces from 77 K to 447 K, respectively. Here, $E_{\rm eff}$ is defined with η of 1/3. It is found that the mobilities on (110) and (111) have almost no temperature dependence over the range of 77 K to 133 K. This fact confirms us that the difference in the $E_{\rm eff}$ dependences at 77 K between on (110) and (111) is ascribed to the different influence of surface roughness scattering. With

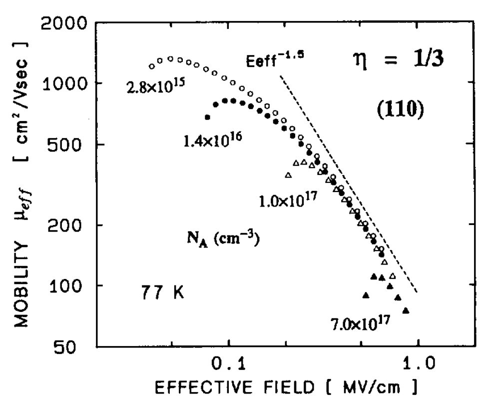

Fig. 3. Electron mobility in inversion layer on (110) at 77 K versus effective field, $E_{\rm eff}$, as a parameter of substrate acceptor concentration, N_A. Here, $E_{\rm eff}$ is defined with η of 1/3.

increasing temperature, on the other hand, the $E_{\rm eff}$ dependence of mobilities on (110) and (111) are found to approach roughly

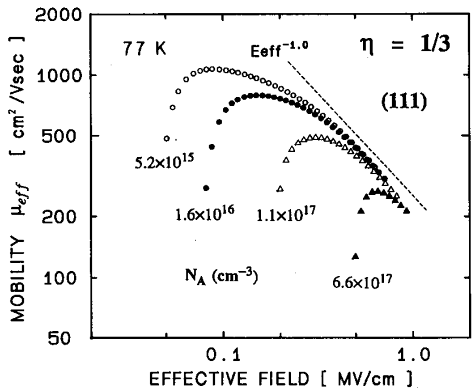

Fig. 4. Electron mobility in inversion layer on (111) at 77 K versus effective field, E_{eff}, as a parameter of substrate acceptor concentration, N_A. Here, E_{eff} is defined with η of 1/3.

TABLE I
VALUES OF η PROVIDING UNIVERSALITY FOR EACH SURFACE ORIENTATION

η	(100)	(110)	(111)
ELECTRON	1/2	1/3	1/3
HOLE	1/3	—	—

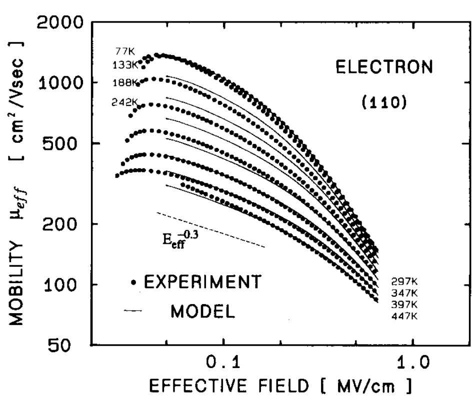

Fig. 5. E_{eff} dependences of electron mobility in inversion layer on (110) surface in the range of 77 K to 447 K. Substrate acceptor concentration is 3.9×10^{15} cm^{-3}. Here, E_{eff} is defined with η of 1/3. Open circles show the experimental data. The solid curves were calculated using (1) and (2).

$E_{\mathrm{eff}}^{-0.3}$, as seen in that on (100). This demonstrates that the mobility limited by phonon scattering, μ_{ph} has the same E_{eff} dependence ($E_{\mathrm{eff}}^{-0.3}$) independent of surface orientations.

On the basis of the above experimental results, it was examined whether the experimental mobilities on (110) and (111) can be described by the combination of μ_{ph} and μ_{sr}. μ_{ph} and μ_{sr} can be simply modeled in the following equations, as in the companion paper [8].

$$\mu_{\mathrm{ph}} = A \cdot E_{\mathrm{eff}}^{-0.3} \cdot T^{-\alpha} \tag{1}$$

$$\mu_{\mathrm{sr}} = \mu_{77K} \tag{2}$$

$$\mu_{\mathrm{tot}}^{-1} = \mu_{\mathrm{ph}}^{-1} + \mu_{\mathrm{sr}}^{-1}. \tag{3}$$

Here, a constant A was taken to be 1.7×10^5 and 1.9×10^5 for on (110) and (111), respectively, where μ, E_{eff} and T should be in cm/V·s, V/m and kelvins. α was taken to be 1.75 for both

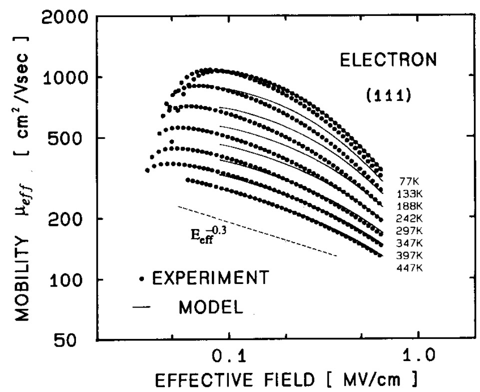

Fig. 6. E_{eff} dependences of electron mobility in inversion layer on (111) surface in the range of 77 K to 447 K. Substrate acceptor concentration was 3.9×10^{15} cm^{-3}. Here, E_{eff} is defined with η of 1/3. Open circles show the experimental data. The solid curves were calculated using (1) and (2).

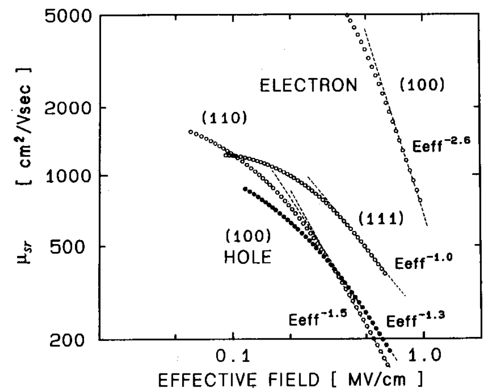

Fig. 7. E_{eff} dependences of the mobilities limited by surface roughness scattering, μ_{sr}, as a parameter of surface orientation or carrier type.

(110) and (111), as same as the case in (100) [8]. The solid lines in Figs. 5 and 6 represent the results calculated using (1)–(3). Although there is a discrepancy near 77 K, a good agreement between the solid lines and the experimental data is obtained above 200 K, indicating that the E_{eff} dependences of the mobilities are explainable by μ_{ph} in (1) and μ_{sr} in (2). The μ_{sr} for electrons on (100), (110), and (111) and for holes on (100) are plotted as a function of E_{eff} in Fig. 7. μ_{sr} on (100) was studied in the common paper [8]. It is seen that the E_{eff} dependence of μ_{sr} varies roughly from $E_{\mathrm{eff}}^{-2.6}$ to E_{eff}^{-1} dependent on surface orientation.

III. DISCUSSION

In the previous section, it has been concluded that the universal curves for electrons on (100), (110), and (111) come from the contribution of two scattering mechanisms, phonon scattering and the surface roughness scattering. Therefore, the physical meaning of E_{eff} and the E_{eff} dependence of the universal curves should be explained for these two mobility components, μ_{ph} and μ_{sr}, separately. In this section, these points are discussed on the basis of the scattering theory in 2DEG.

A. Phonon Scattering

Under the assumption that carriers in the inversion layer are 2DEG and occupy only the lowest subband, the mobility determined by acoustic phonon scattering is described as follows [12], [13].

$$\mu_{\rm ph} = \frac{q}{m_c} \cdot \frac{\hbar^3 \rho s_l^2}{m_d D_{\rm ac}^2 k_B T} \cdot W \tag{4}$$

$$W = \left(\int |\xi(z)|^4 dz \right)^{-1}. \tag{5}$$

Here, m_c is the conductivity mass parallel to surface, m_d is the density-of-state mass parallel to surface, $D_{\rm ac}$ is the deformation potential energy for acoustic phonon, ρ is the density of Si, s_l is the sound velocity in Si and $\xi(z)$ is the envelope function of two dimensional carriers. W in (5) is the effective width of the inversion layer and, thus, is dependent on the form of the wave function. Using the wave function of Stern and Howard [9] as $\xi(z)$,

$$W = \frac{16}{3} \left(\frac{\varepsilon_{\rm Si} \hbar^2}{12 m_3 q^2} \right)^{1/3} \cdot \left(N_{\rm dpl} + \frac{11}{32} N_s \right)^{-1/3}. \tag{6}$$

As a result, the mobility given by (4) has the universality against $E_{\rm eff}(= q(N_{\rm dpl} + \eta \cdot N_s)/\epsilon_{\rm Si})$ with η of 11/32, and is in proportion to $E_{\rm eff}^{-1/3}$ in the quantum limit. It should be noted that the term of $(N_{\rm dpl} + \eta \cdot N_s)$ comes from W, the effective width of the inversion layer.

As shown in Table I, the experimental values in η for the electron mobility on (110) and (111) and the hole mobility on (100) and 1/3, which is almost the same as 11/32. Moreover, the experimental $E_{\rm eff}$ dependence of $\mu_{\rm ph}$ is roughly $E_{\rm eff}^{-0.3}$, which is almost the same as that $E_{\rm eff}^{-1/3}$. Thus, the universality of $\mu_{\rm ph}$ for electrons on (110) and (111) and holes on (100) can be understood by acoustic phonon scattering under the single subband occupation.

In contrast, the electron mobility on (100) has the universality with $\eta = 1/2$. This deviation of the η from 11/32 may come from the fact that the electrons in the inversion layer on (100) occupy more subbands at room temperature, and so that the assumption of single subband occupation in (4) does not hold. The inversion layer on (100) has the two different ladders in the subband structure and, moreover, the density of state of the lowest subband is the smallest among the three orientations. These characteristics of the subband on (100) lead to the smaller carrier occupancy of the lower subband, which had already been confirmed by the self-consistent calculations [14]. According to this calculation (Fig. 6 in [14]), the fractions in the lowest subband on (100) at 300 K is approximately as low as 20% at N_s of 1×10^{12} cm^{-2}, while those on (110) and (111) are 40 and 60%, respectively. Although the occupancy of the lowest subband becomes larger with an increase in N_s, the amount of the occupancy on (100) keeps being the smallest. We think that the deviation of η from 1/3 on (100) surface can be attributed to the occupation of higher subbands on (100). On the other hand, the value of γ on (100) is still -0.3, which is the same as (110) and (111). This result suggests that the $E_{\rm eff}$ dependence of $\mu_{\rm ph}$ is little affected by the multi-subband occupation.

As for the temperature dependence of $\mu_{\rm ph}$, the experimental dependence is $T^{-1.75}$, which is stronger than that given theoretically by (4), T^{-1}. This fact is attributable to the contribution of intervalley phonon scattering [13], which is known to provide much stronger temperature dependence because of the higher energies of the relevant phonons. It should be noted here that the mobility limited by intervalley phonon scattering is also in proportion to W in (5) under the single subband occupation [13]. Therefore, the interpretation for the universality, based on (4)–(6), still holds under the influence of intervalley phonon scattering.

B. Surface Roughness Scattering

The theoretical formulation for the relaxation time of surface roughness scattering, $\tau_{\rm sr}(k)$, has been given by Matsumoto and Uemura [15]. Under the assumption of single subband occupation, $\tau_{\rm sr}(k)$ can be described by

$$\tau_{\rm sr}^{-1}(k) = \frac{q^2 m_d}{\pi \hbar^3} \cdot E_{\rm av}^2 \int_0^\pi d\theta (1 - \cos\theta) S\left(2k \cdot \sin\frac{\theta}{2}\right) \tag{7}$$

$$S(q) = \int \Delta(r) \exp(-iqr) dr \tag{8}$$

$$E_{\rm av} = \frac{q}{\varepsilon_{\rm Si}} \left(N_{dpl} + \frac{1}{2} N_s \right). \tag{9}$$

Here, $\Delta(r)$ is the autocorrelation function of interface roughness and k is the wave vector of electrons in the inversion layer. It is generally assumed that $\Delta(r)$ is Gaussian type function, $\Delta^2 \exp(-r^2/L^2)$, where Δ and L are the height and the correlation length of interface roughness, respectively. Then, (7) is

$$\tau_{\rm sr}^{-1}(k) = \frac{q^2 m_d \Delta^2 L^2 E_{\rm av}^2}{\hbar^3} \times \int_0^\pi d\theta (1 - \cos\theta) \exp\left(-\frac{1}{2} L^2 k^2 (1 - \cos\theta) \right). \tag{10}$$

In this formulation, $E_{\rm av}$ means the normal field averaged over the inversion layer. If we consider this $E_{\rm av}$ as $E_{\rm eff}$, the value of η is to be 1/2. Note that this coefficient in $E_{\rm av}$ is strictly 1/2 even under the multi-subband occupation, according to the theoretical formulation [10], [15]. In the limit that the correlation length is much smaller than electron wave length ($L \ll k^{-1}$), the mobility limited by surface roughness scattering, $\mu_{\rm sr}$, is simply represented as follows [15].

$$\mu_{\rm sr} = \frac{\hbar^3}{\pi q m_d m_c} \cdot (\Delta L E_{\rm av})^{-2}. \tag{11}$$

As a result, when we interpret $E_{\rm av}$ in (11) as $E_{\rm eff}$, $\mu_{\rm sr}$ should have the universality for $E_{\rm eff}$ with η of 1/2 and is proportional to $E_{\rm eff}^{-2}$.

It has been obtained experimentally that $\mu_{\rm sr}$ for electrons on (100) has η of 1/2 and is in proportion to $E_{\rm eff}^{-2.6}$, as shown in Fig. 7. Therefore, $\mu_{\rm sr}$ on (100) can be understood by (11), although the experimental $E_{\rm eff}$ dependence is somewhat stronger. However, the experimental $\mu_{\rm sr}$ for electrons on (110) and (111) and for holes on (110) cannot be explained by

(11), because the experimental value of η is 1/3 and the E_{eff} dependence ($E_{\mathrm{eff}}^{-1.5} \sim E_{\mathrm{eff}}^{-1.0}$) is rather weaker than in (11). This weaker E_{eff} dependence cannot be explained by changing Δ and L within the framework of (11), though it has been reported [16] that the values of Δ and L estimated from μ_{sr} are dependent on surface orientations.

On the other hand, if L is not sufficiently small, μ_{sr} cannot be described only by E_{eff} with η of 1/2 but deviates from the dependence of E_{eff}^{-2}, because the integral term in (10) has the N_s dependence. Therefore, in order to correctly examine whether the formulation of (10) can explain the experimental results on (110) and (111) or not, the theoretical mobility including the effect of the integral term should be compared with the experimental data. Since (10) is, to our knowledge, the only one formulation for surface roughness scattering and commonly used in the analysis of μ_{sr} [10], [13], [16]–[18], it is quite important to clarify the applicability of (10).

The calculated N_s dependence and temperature dependence of μ_{sr} on (111) are shown in Figs. 8 and 9. μ_{sr} was calculated by integrating $\tau_{\mathrm{sr}}(k)$ given by (10) over Fermi–Dirac distribution with respect to electron energy of a 2DEG. Here, the substrate impurity concentration was taken to be as low as 10^{15} cm^{-3} and, thus, the N_s dependence is the same as E_{eff} dependence. It is found in Fig. 8 that, with an increase in L, the N_s dependence becomes weaker than N_s^{-2}, suggesting that the experimental weaker E_{eff} dependence is explainable by taking the value of L to be more than 30 Å. This result comes from the fact that electrons with wave lengths shorter than L are scattered less frequently. However, as shown in Fig. 9, the temperature dependence of the calculated μ_{sr} with larger L is not in agreement with that of the experimental μ_{sr}. μ_{sr} with larger L is found to increase with an increase in temperature significantly. This is because with increasing temperature the averaged wave length of electrons decreases under the Fermi-Dirac statistics, and, as a consequence, the scattering rate becomes lower. The above results demonstrate that, even if the value of L changes, it is difficult to consistently explain both the experimental E_{eff} dependence and the temperature dependence within the framework of (10). The theoretical formulation of (10) has been so far successful to describe μ_{sr} on (100) under the reasonable values of L and Δ[10], [13], [16]–[18]. However, the finding in this study that this formula is not necessarily applicable to μ_{sr} on (110) and (111) demands the refinement and reexamination of this formulation.

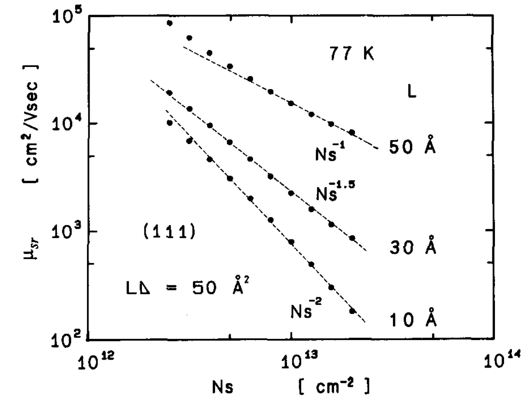

Fig. 8. Calculated N_s dependences of electron mobility limited by surface roughness scattering, μ_{sr}, at 77 K on (111). A parameter is a correlation length of interface roughness between Si and SiO_2, L. Here, $L \cdot \Delta$ is fixed at 50 Å^2 for each L. Dash lines are drawn for guiding eyes in comparison with the experimental E_{eff} dependence. In the calculation $\Delta \cdot L$ was fixed at 50 Å^2 in order to extract only the effect of L on μ_{sr}, because μ_{sr} should be described as a function of $\Delta \cdot L$, if the influence of the integral term is negligible.

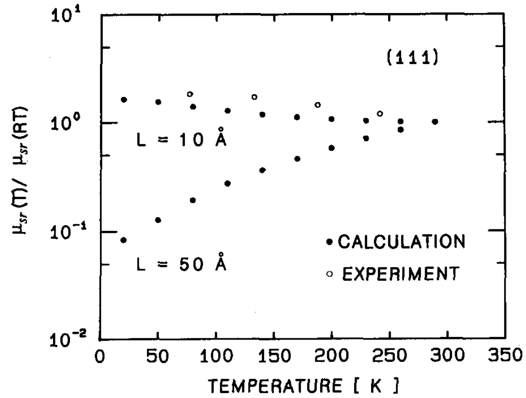

Fig. 9. Normalized temperature dependences of calculated μ_{sr} at N_s of 10^{13}cm^{-2} for L of 10 Å and 50 Å. The mobility is normalized by the value at 290 K. In comparison, the experimental mobility at N_s of 10^{13} cm^{-2} is also plotted.

IV. Conclusion

The inversion layer electron mobilities on the different surface orientations, (100), (110), and (111) surfaces, have been studied from the viewpoint of the universal relationship. It has been found for the first time that the mobilities on (110) and (111) have also the universal relationship against the E_{eff} and that the value of η in the E_{eff} is dependent on surface orientation. The value of η is 1/3 for the electron mobilities on (110) and (111), instead of 1/2 on (100). This result has been qualitatively explained by considering the difference of the subband occupancy for these surface orientations. It has been found that μ_{ph} has the same E_{eff} dependence, $E_{\mathrm{eff}}^{-0.3}$, among the three orientations. On the other hand, the E_{eff} dependence of μ_{sr} is different significantly among the three orientations and becomes weaker in the order of (100), (110), and (111). While the theoretical formulation of surface roughness scattering, used currently, explains the behavior of μ_{sr} on (100), it has been found that it fails to describe μ_{sr} on (110) and (111), with any choice of the roughness parameters, L and Δ, demanding the further refinement of the theoretical formulation.

Acknowledgment

The authors wish to thank M. Yoshimi, K. Natori, and T. Wada for their encouragement throughout this work.

References

[1] A. G. Sabnis and J. T. Clemens, in *IEDM Tech. Dig.*, pp. 18–21, 1979.
[2] S. C. Sun and J. D. Plummer, *IEEE Trans. Electron Devices*, vol. ED-27, pp. 1497–1508, 1980.
[3] N. D. Arora and G. S. Gildenblat, *IEEE Trans. Electron Devices*, vol. ED-34, pp. 89–93, 1987.

[4] J. T. Watt and J. D. Plummer, in *Symp. on VLSI Technol. Tech. Dig.*, 1987, pp. 81–82.
[5] S. Takagi, M. Iwase, and A. Toriumi, in *IEDM Tech. Dig.*, 1988, pp. 398–401.
[6] S. Takagi, M. Iwase, and A. Toriumi, in *Ext. Abstracts 22nd Conf. Solid State Devices and Materials*, 1990, pp. 275–278.
[7] C. L. Huang and G. Sh. Gildenblat, *IEEE Trans. Electron Devices*, vol. 37, pp. 1289–1300, 1990.
[8] S. Takagi, A. Toriumi, M. Iwase, and H. Tango, *IEEE Trans. Electron Devices*, vol. 41, pp. 2357–2362.
[9] F. Sten and W. E. Howard, *Phys. Rev.*, vol. 163, pp. 816–835, 1967.
[10] T. Ando, A. B. Fowler, and F. Stern, *Rev. Mod. Phys.*, vol. 54, pp. 437–672, 1982.
[11] T. Sato, Y. Takeishi, H. Hara, and Y. Okamoto, *Phys. Rev. B*, vol. B4, pp. 1950–1960, 1971.
[12] P. J. Price, *Annu. Phys.*, vol. 133, 1981, pp. 217–239.
[13] K. Masaki, C. Hamaguchi, K. Taniguchi, and M. Iwase, *Jpn. J. Appl. Phys.*, vol. 28, pp. 1856–1863, 1989.
[14] F. Stern, *Phys. Rev. B*, vol. B5, pp. 4891–4899, 1972.
[15] Y. Matsumoto and Y. Uemura, *Jpn. J. Appl. Phys. Suppl. 2*, pt. 2, pp. 367–370, 1974.
[16] K. Lee, J. S. Choi, S. P. Sim and C. K. Kim, *IEEE Trans. Electron Devices*, vol. 38, pp. 1905–1912, 1991.
[17] D. K. Ferry, in *IEDM Tech. Dig.*, 1984, pp. 605–608.
[18] S. M. Goodnick, D. K. Ferry, C. W. Wilmsen, Z. Lilienthal, D. Fathy, and O. L. Krivanek, *Phys. Rev. B*, vol. B32, pp. 8171–8186, 1985.

Shin-ichi Takagi (M'93), for a photograph and biography, please see this issue, page 2362.

Akira Toriumi, for a photograph and biography, please see this issue, page 2362.

Masao Iwase, for a photograph and biography, please see this issue, page 2362.

Hiroyuki Tango, for a photograph and biography, please see this issue, page 2362.